Distortion of Visible Daytime Multi-Conjugate Adaptive Optics Control

Puttiwat Kongkaew[a], Timothy J. Morris[a], and James Osborn[a]

[a]Centre for Advanced Instrumentation, Department of Physics, Durham University, South Road, Durham, DH1 3LE

ABSTRACT

Daytime optical observations, including solar telescope and free-space optical communication, experience strong turbulence and scintillation. These conditions cause control problems in Multi-Conjugate Adaptive Optics (MCAO). Considering an MCAO setup with two deformable mirrors (DMs) and wavefront sensors (WFSs), when the system is active, downstream DM distorts image and control of upstream DM at WFSs. Scintillation and shift in position of upstream DM's actuator at the WFSs induced by active downstream DM are major error sources. Distorted control of upstream DM was simulated including propagation effect with downstream DM correcting a turbulence layer. With flattened downstream DM, upstream DM with distorted control was used to correct a static turbulence. Regions with log-amplitude variance between 0.1 and 0.3 and actuator statistical shift between 10% and 50% WFS subaperture may have partial correction. Regions with extremely low and high distortion have no impact in performance and no AO correction, respectively.

Keywords: Multi-conjugate Adaptive Optics, Scintillation, Control, Wave propagation

1. INTRODUCTION

Performance of daytime Multi-Conjugate Adaptive Optics (MCAO) is degraded by pupil distortion which can appear in forms of scintillation and distortion of geometry of adaptive optics control (AO).[1] Stronger atmospheric turbulence conditions such as those encountered during daytime, at low-elevation angles, or in sites at a low altitude will encounter stronger scintillation and distortion. This situation is applicable to solar astronomy and free-space optical communications.

MCAO simulation studies have shown low AO correction at 8cm r_0,[1] and daytime turbulence can even at good observing sites, have r_0 between 2-4cm.[2–4] Even though distortion of the AO control geometry i.e. the geometry between a wavefront sensor and deformable mirror was noticed and attempted to minimized through regularization of AO control, it was not analyzed.[1]

Let's define deformable mirror (DM)'s naming convention based on order of DMs within MCAO; DM1 and DM2 are the first and second DMs respectively, Figure 1. During AO operation, DM2 will be applying some turbulence correction, introducing phase distortion to image of DM1. As a result image of DM1 and its effective actuator positions at the WFS will be distorted, Figure 2. Consequently, AO control is also distorted degrading MCAO performance.

2. SOURCES OF DISTORTIONS

2.1 Adaptive Optics Close Loop Control

In order to control adaptive optics in a close loop, interaction or conversion between DM and WFS must be measured. The interaction is mostly represented by matrices. Changes in WFS slopes corresponding to each DM actuator is called interaction matrix; in other words, given DM actuator strokes what are WFS slopes. The pseudo-inverse of interaction matrix is control matrix; given changes in WFS slopes what are DM strokes.

Further author information: (Send correspondence to P.K.)
P.K.: E-mail: puttiwat.kongkaew@durham.ac.uk, Telephone: +44 (0)19 1334 4746

Adaptive Optics Systems IX, edited by Kathryn J. Jackson, Dirk Schmidt, Elise Vernet,
Proc. of SPIE Vol. 13097, 130975U · © 2024 SPIE · 0277-786X
doi: 10.1117/12.3019648

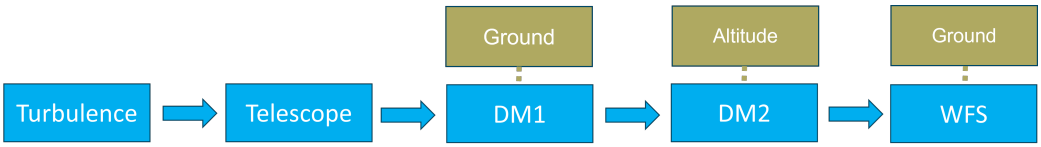

Figure 1. Shows block diagram of light path through each principal components in an MCAO system by order of precedence. We defined DM1 as the first DM in light path and DM2 as the second. Conjugation of DM1 and DM2 may varies from design to design. For this study, DM1 and WFSs are conjugated to ground layer turbulence, while DM2 is conjugated to altitude turbulence.

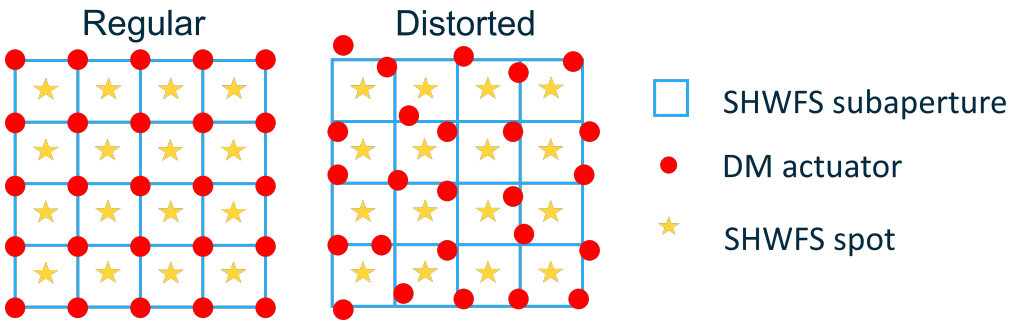

Figure 2. Sketch showing the Fried geometry between DM1 actuators and WFS when DM2 is held flat e.g. during calibration (left) where actuators are positioned on the corner of SHWFS subaperture, and during operation when geometry becomes distorted by DM2 (right) where the apparent actuator positions are randomly shifted away from corners of SHWFS subaperture.

Interaction matrices of DM is generated by measuring difference in WFS slopes before and after poking of an actuator. Stacks of WFS slope differences is the interaction matrix. Linear relation between adjustment in DM strokes (a), WFS residual slope measurement (s) and interaction matrix ($\mathbf{IM}$) can be written as[5]

$$s = \mathbf{IM}a. \tag{1}$$

Solution for DM actuator strokes for given WFS slopes can be solved linear algebraically with pseudo-inverse (noted by $^+$ operator) matrix of interaction matrix called control matrix ($\mathbf{CM}$).[6]

$$\mathbf{CM} = \mathbf{IM}^+ \tag{2}$$

$$a = \mathbf{CM}s \tag{3}$$

Pseudo-inverse can be calculated by singular value decomposition method (SVD),[5] requiring a normalized conditioning parameter.[7] The optimized conditioning parameter for pseudo-inverse can be chosen by comparing AO performance. The conditioning value yielding the highest Strehl ratio is chosen.

Strehl ratio is defined as ratio of maximum intensity in point-spread-function (PSF) profile between image with (I) and without aberrations (I_0).[8]

$$S/ = \frac{I}{I_0} \tag{4}$$

In this study a close loop control of adaptive optics is used. At time $t+1$ DM actuator commands (a_{t+1}) depend on WFS measures wavefront residues (s_t) and DM commands (a_t) at time t, as follow.[6]

$$a_{t+1} = a_t - g\mathbf{CM}s_t, \tag{5}$$

where g is control loop gain.

Adaptive optics control is closely tied to image of DM at WFS. Any distortion to DM image will also distort the control. The distortion can be quantified into either using distortions of phase and intensity due to optical propagation and scintillation, or geometry based on the observed displacement of actuator positions. Both these effects are dependent on a similar set of parameters, and here we wish to determine boundary conditions where pupil distortion might have no effect, partial effect, or imminent effect on AO performance.

2.2 Optical Propagation and Scintillation

Light diffracts as it propagates over distance. The effect is normally not considered in AO system design for near-infrared astronomy, because its effect is negligible in longer wavelength and weaker turbulence. In situations where stronger turbulence can be encountered such as solar astronomy and free-space optical communications, or operation at very short wavelengths, optical propagation through optical turbulence must be included. The spatial solution to optical wave can be written in phasor form as:[9]

$$U = Ae^{i\phi} = \sqrt{I}e^{i\phi} = e^{\chi+i\phi}, \tag{6}$$

where U is complex amplitude of the wave, A is amplitude, e is Euler's number , i is imaginary unit, ϕ is phase, and χ is log-amplitude. Intensity (I), amplitude (A), and log-amplitude (χ) are related as follows:

$$\chi = \ln(A) = \frac{\ln(I)}{2}. \tag{7}$$

Atmospheric optical turbulence can be profiled by distribution of turbulent layers, each with a strength (C_n^2) at different altitude from the ground (h). When an observation is made at a zenith distance (ζ), the optical distance from telescope pupil (z) is[9]

$$z = h \sec\zeta \tag{8}$$

Total turbulence strength in a line of sight is parameterized by coherence length or Fried parameter (r_0). If we define k_0 be the wavenumber, r_0 relates to C_n^2 by:[9]

$$r_0 = \left(0.423k_0^2 \int C_n^2(h)\sec\zeta dh\right)^{-3/5}. \tag{9}$$

As light propagates through and beyond an optical turbulence layer the intensity of light will become non-uniform. The variation in intensity and other related terms are called scintillation. The scintillation is commonly studied in the form of variation of log-amplitude (σ_χ^2) which is called the scintillation index. Scintillation through turbulence can be calculated using Rytov's approximation, Equation 10.[9] Even though the approximation is valid from 0-0.25,[9] it can be used as a marker for AO analysis.[10,11] Scintillation indices shown in this work are scintillation induced by DM2. It is calculated from the Rytov approximation and not always the same value of what exist in the simulation. The Rytov approximation is

$$\sigma_\chi^2 = 0.5631k_0^{7/6}\sec^{11/6}\zeta \int C_n^2(h)h^{5/6}dh, \tag{10}$$

An example of the evolution of both the optical phase and intensity propagating a distance from an optical turbulence is shown in Figure 3. The propagation distance has been increased to show different scintillation indices. When $\sigma_\chi^2 > 0.2$, wavefront sensor measurements may become inaccurate.[11] Analytical solutions to propagation through turbulence using smooth perturbation start to fail at $\sigma_\chi^2 = 0.35$.[9] The scintillation becomes saturated, at $\sigma_\chi^2 = 0.6$[9] (phase tends to be uniformly distributed, resulting in maximum variation in intensity), setting an upper limit where scintillation effect becomes dominant and may result in no AO correction.

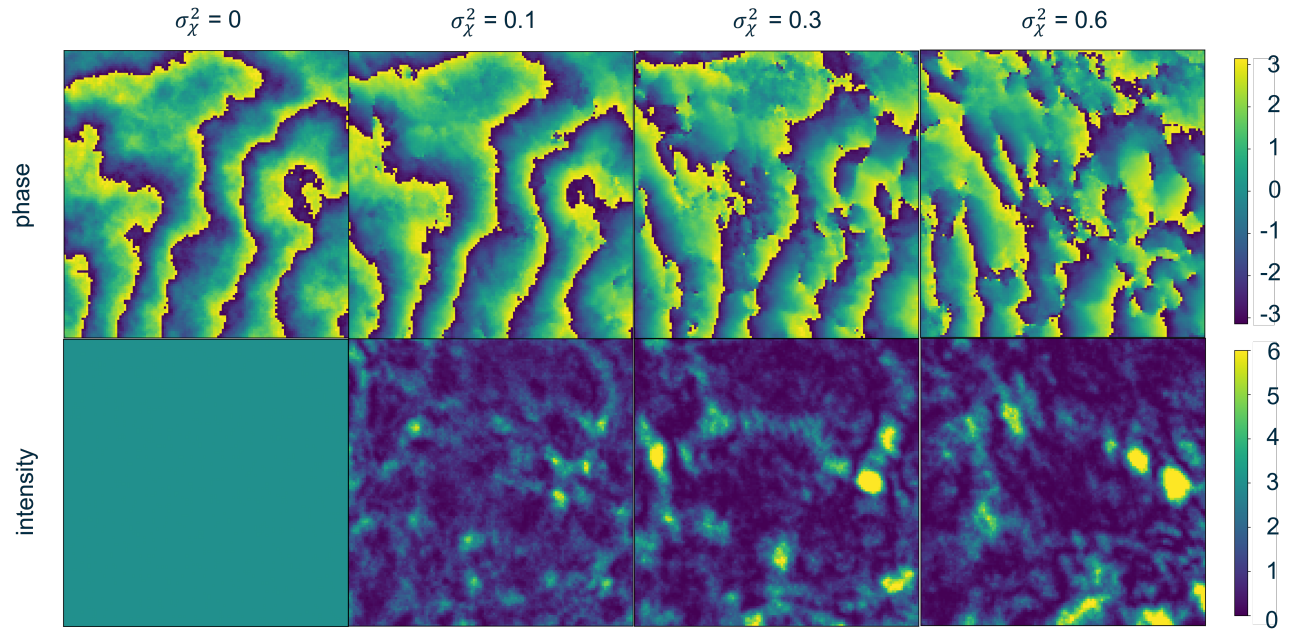

Figure 3. Phase in radians (top) and normalized intensity (bottom) of a 500nm, 40cm aperture, 5cm r_0 turbulence as it propagates down a line of sight at increasing Rytov's approximation (σ_χ^2).

2.3 Geometric Pupil Distortion

Misregistration or actuator shift effect on AO calibration in scintillation free case has been studied for many AO systems (see e.g.[12,13]), using static shifts or rotations between WFS and DM. For the sensing and correction of atmospheric optical turbulence, it is commonly understood that misregistration or rotation that introduces a wavefront sensor shift of greater 10-30% of an subaperture diameter will start to impact AO performance.[14,15] In this study, the source of misregistration is not caused by misalignment in hardware, but rather the distortion. Distortion of a DM pupil in daytime MCAO was observed[16] which changes registration between DM and SHWFS[17] dynamically, depicted in Figure 2. Pupil distortion was presented using shift of DM actuators away from its Fried geometry grid-like pattern.[1] To estimate the RMS amplitude of the geometric pupil distortion caused by a non-conjugated deformable mirror we can use the definition of wavefront angle-of-arrival due to optical turbulence (α_{jit}) across a WFS subaperture. The root-mean-square (RMS) of angle-of-arrival statistics over a circular aperture is given by:[18]

$$\alpha_{jit} = \sqrt{0.182\lambda^2 D^{-1/3} r_0^{-5/3}}, \tag{11}$$

where λ is wavelength, D is aperture size. For calculating actuator shift due to an intermediate deformable mirror we assume r_0 describes the turbulence strength being corrected by the deformable mirror (DM2). Furthermore, aperture size (D) is replaced by the WFS's subaperture size (d_s).

The geometric pupil distortion is the angle of arrival multiplied by the conjugate distance between the WFS and the intermediate DM2 which we call H, $\alpha_{jit}H$. To provide a direct comparison to misregistration effects, we then scale the geometric pupil distortion by the subaperture size to define the actuator shift, AS, statistical displacement of centre of DM1's pokes compared to its usual Fried geometry position:

$$AS = \frac{\alpha_{jit}H}{d_s} = H\sqrt{0.182\lambda^2 d_s^{-7/3} r_0^{-5/3}}. \tag{12}$$

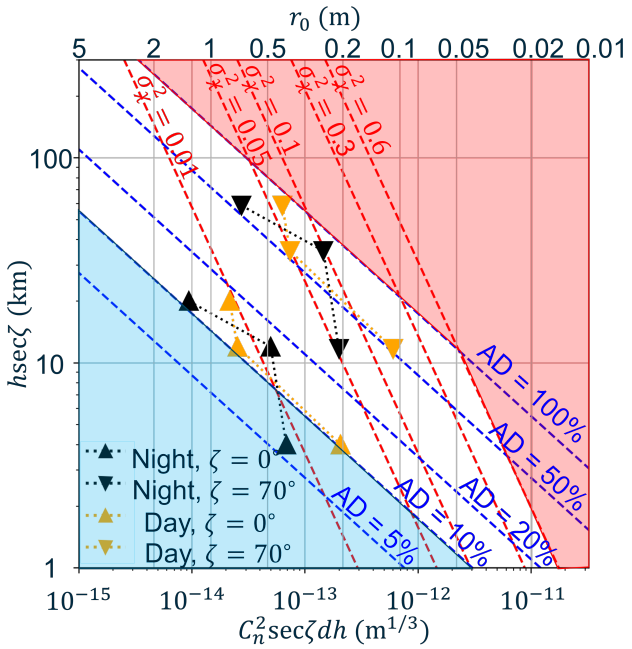

Figure 4. Shows region of AO operations expected to have negligible (blue / lower left shaded) and strong distortion (red / upper right shaded). Values are calculated for 5cm subaperture geometry at 500nm. X-axis shows turbulence strength being corrected by DM2. Y-axis shows altitude difference between DM1 and DM2. Contour plots of scintillation indices (red dashed with σ_χ^2 labeled) and relative actuator shift (blue dashed with AS labeled) are overlaid. Turbulence profiles (dotted lines) of the stronger 3rd Quartile from 24h SHIMM data at Paranal[2] both during the night (black) and the day (yellow) and looking at zenith (pointed up triangle) and 70 degrees (pointed-down triangle) from the zenith are shown for comparison

3. ADAPTIVE OPTICS SYSTEM CONFIGURATIONS IN EFFECT

Scintillation effects vary with wavelength, turbulence strength, and propagation distance. The resulting dynamic geometric actuator shift (AS) observed in a multiple deformable mirror system does vary similarly but we expect its effect to also scale with subaperture size, in line with more classic definitions of static WFS to DM misregistration. Simulations of a 2-layer MCAO operation with a fixed SHWFS operating wavelength and subaperture size were implemented to study this effect. Figure 4 shows in which regimes we expect pupil distortion and scintillation effects to impact AO system performance. On the X-axis Figure 4 plots layer turbulence strength in a layer ($C_n^2 \sec\zeta dh$) against propagation distance between DM1 and DM2 ($h \sec\zeta$). Scintillation index (σ_χ^2) and actuator shift (AS) are shown in contours. Turbulence profiles at different zenith angles (ζ) can be overlaid. For this study, 5-cm SHWFS subapertures and a 500nm operating wavelength are chosen. Let DM1 and DM2 correct ground layer (GL) and high altitude (HA), respectively. Regions in Figure 4 can be provisionally categorized into three regions where DM1 distortions are supposedly negligible ($\sigma_\chi^2 < 0.1$ and $AS < 10\%$), dominant ($\sigma_\chi^2 > 0.6$ or $AS > 100\%$), and noticeable (in between). The values are inspired loosely from discussions in the previous section.

Figure 4 shows in red the scintillation regimes where an AO system with 5cm WFS sampling would likely not provide correction when actuator shift (AS) $> 100\%$ or scintillation index (σ_χ^2) > 0.6. This is observed in strong turbulence conditions when DM conjugation separations (H) at 10km which can be the case for solar AO systems. This is unlikely to be a configuration encountered for night-time AO, unless WFS subaperture diameters are reduced to 5cm used here. WFS subaperture diameters of 2cm would observe an actuator shift of 50% at DM conjugate separations of 4.3km.

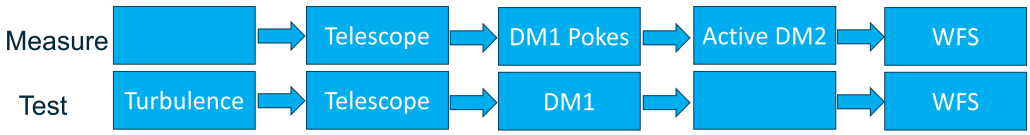

Figure 5. Optical components in simulation during measurement of distorted interaction matrices of DM1 and test for distorted interaction matrices performance.

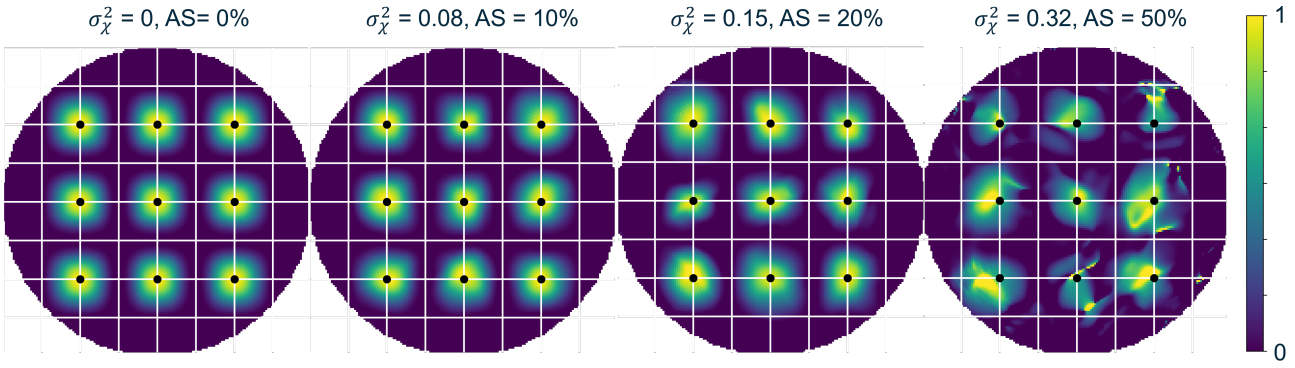

Figure 6. Distorted phase of DM1 actuator pokes at 500nm at the WFS with 5 cm subapertures through active DM2 which is correcting 5cm r_0 turbulence for increasing relative actuator shift (AS) to SHWFS subaperture size. Phase are normalized to poke values.

4. METHOD

To model effect of interaction matrix distortion on AO performance, we have implemented an AO simulation incorporating optical propagation between DMs and WFS. Propagation distance ($h \sec\zeta$) and turbulence strength ($C_n^2 dh \sec\zeta$) are chosen based on intersections of actuator shift (AS) and scintillation index (σ_χ^2) as shown in Figure 4. DM1 and DM2 is conjugated to ground and altitude, respectively. Distorted IMs are measured by 'calibrating' DM1 through a random static DM2 applying Kolmogorov turbulence with only spatial frequency lower than half frequency of SHWFS. Then DM1's distorted IMs are tested to correct 5cm r_0 ground turbulence with flatten DM2 in a close loop control. WFS with 5cm subaperture at 500nm is used. Schematics of IMs measurement and test are shown in Figure 5. Conditioning parameter to pseudo-invert interaction matrices, distorted and undistorted alike, are optimized with respect to undistorted interaction matrix performance. Control gain (g) equal to 0.5 is used throughout this study.

5. INITIAL RESULTS

5.1 Distortion of Interaction Matrices

Effect at WFS of DM1 actuator pokes through DM2 correcting some turbulence are distorted when the proposing distortion parameters increase as shown in Figure 6. Consequently, instantaneous interaction matrix of DM1 is also distorted. Distorted interaction matrices of DM1 by active DM2 is measured, sampling on scintillation index (σ_χ^2) and actuator shift (AS) spaces as shown in Figure 7. Interaction matrices shows stronger distortion as both of the proposed distortion sources increase. The difference between distorted and undistorted interaction matrices of DM1 by DM2 are measured, using only major slope responses (the brighter ones in Figure 7). The error for $\sigma_\chi^2 = 0.1$ & $AS = 10\%$, on the edge between the expected-unaffected regions in AO performance (blue) and expected-affected region (white) in Figure 4, is 11%. In the expected-affected (white) region in Figure 4, for $\sigma_\chi^2 = 0.1$ & $AS = 50\%$, which is has 34% error, while it is 46% for $\sigma_\chi^2 = 0.3$ & $AS = 50\%$. These errors in interaction matrices as distortion parameters increase agree with the hypothesis.

5.2 Control Error

To assess the impact of the distortion on AO correction, the intermediate DM is then removed from the simulation, and the distorted interaction/control matrices are used to provide AO correction of a static phase screen. Figure

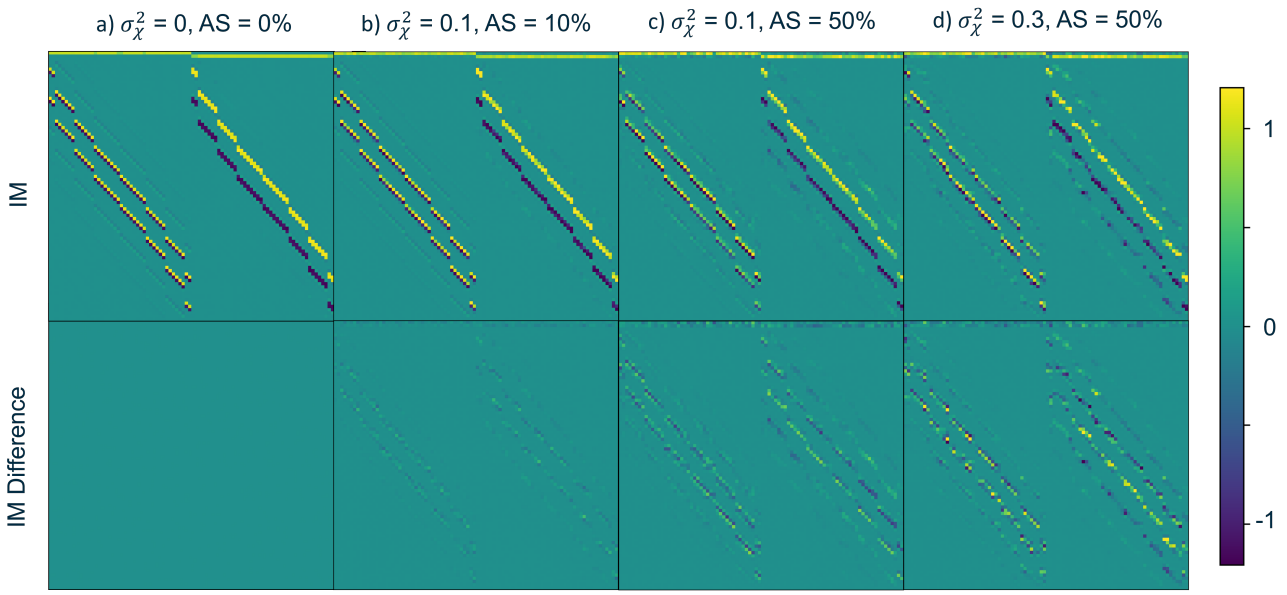

Figure 7. Distorted interaction matrices from DM1 (top) and the difference from the non-distorted interaction matrices (bottom) for increasing distortion of AO geometry (scintillation indices and relative actuator shift (AS) to SHWFS subaperture size). Simulations used 5cm subapertures at 500 nm.

8 shows the instantaneous Strehl ratio when distorted and undistorted control matrices are used to correct a static phase screen with an r_0 of 5cm.

AO performance for $\sigma_\chi^2 = 0.1$ & $AS = 10\%$ which is on the edge of expected-unaffected region (blue / lower left shade) in Figure 4 is indeed unaffected. In addition, AO performance for $\sigma_\chi^2 = 0.6$ & $AS = 100\%$ which is on the edge of expected-no-correction region (red / upper right shade) in Figure 4 indeed has no correction. AO cases in the expected-affected region (white / unshaded) in Figure 4 shows decreasing performance as distortion indices increase. However, with an exception. Sampling in Figure 8 with $\sigma_\chi^2 = 0.3$ and $AS = 10\%$ may shows lower impact on AO performance because it requires DM2 to correct 1cm r_0 turbulence which is much smaller than system's Fried geometry spacing; thus DM2 actuator spacing cannot provide larger spatial frequency turbulence.

Lastly, with minor reduction in AO performance, scintillation index (σ_χ^2) less than 10%, actuator shifts (AS) of up to 50% can be tolerated – far greater than the canonical 10%[14] of a WFS subaperture typically allowed for misregistration, agreeing with a scintillation free study with pyramid WFS.[15] Distortion induced from scintillation index has larger impact on performance of interaction matrices.

6. CONCLUSION

These results show that the distortion of an interaction matrix by an intermediate DM can limit performance for AO systems with multiple deformable mirrors with conjugate separations larger than 10km with WFS subaperture sizes of 5cm, for MCAO configuration with intermediate DM conjugated to altitude. We have used the actuator shift (based on angle of arrival statistics) and scintillation index to describe when this effect may be encountered. Scintillation index is a better indication of when this may occur than the actuator shift, based on angle of arrival statistics.

7. FUTURE WORK

Similar analysis for the opposite MCAO configuration where DM1 and DM2 are conjugate to altitude and ground respectively can be done to confirm if there is any difference in choice of the configuration. Further characterizing effects of each Zernike modes on DM2 maybe beneficial. Since degradation of AO performance is larger than the sampling points, a finer sampling might reveal a clearer behavior. Lastly method to mitigate the control error such as updating the distorted interaction matrices can be studied.

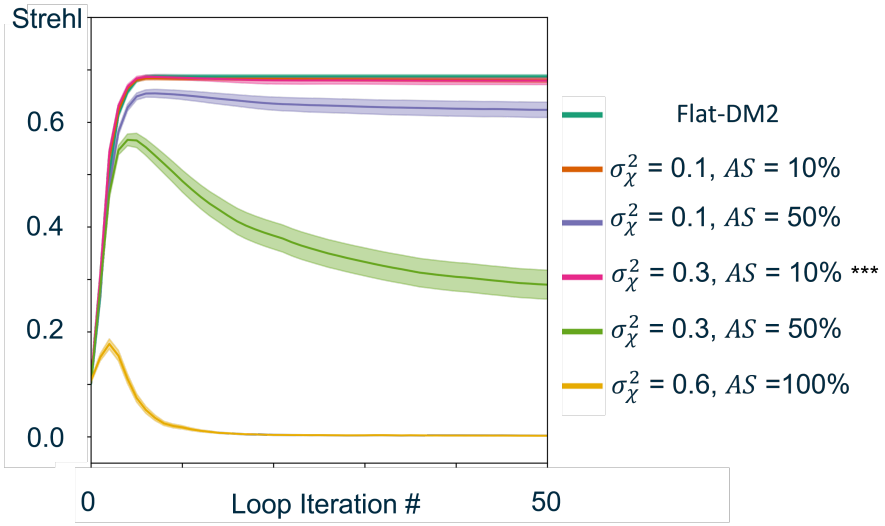

Figure 8. Mean instantaneous Strehl ratio from using distorted interaction matrices of DM1 to correct static 5cm r_0 turbulence. Error bar shows standard error of the mean from 100 simulations. ***Note: for $\sigma_\chi^2 = 0.3$ & $AS = 10\%$, since DM2 with 5cm spacing is correcting 1cm r_0 turbulence, it has low control error.

ACKNOWLEDGMENTS

Puttiwat Kongkaew's PhD. is funded by National Astronomical Research Institute of Thailand (NARIT), Ministry of Higher Education, Science, Research and Innovation (MHESI), the Royal Thai Government, Thailand.

REFERENCES

[1] van Dam, M. A., Hernando, Y. M., Cagigal, M. N., and Montoya, L. M., "Overcoming the effect of pupil distortion in multiconjugate adaptive optics," in [*Adaptive Optics Systems VII*], Schreiber, L., Schmidt, D., and Vernet, E., eds., **11448**, 114480P, International Society for Optics and Photonics, SPIE (2020).

[2] Griffiths, R., Bardou, L., Butterley, T., Osborn, J., Wilson, R., Bustos, E., Tokovinin, A., Le Louarn, M., and Otarola, A., "A comparison of next-generation turbulence profiling instruments at Paranal," *Monthly Notices of the Royal Astronomical Society* **529**(1), 320–330 (2024).

[3] Kellerer, A., Gorceix, N., Marino, J., Cao, W., and Goode, P. R., "Profiles of the daytime atmospheric turbulence above big bear solar observatory," *Astronomy & Astrophysics* **542**(A2) (2012).

[4] Song, T., Cai, Z., Liu, Y., Zhao, M., Fang, Y., Zhang, X., Wang, J., Li, X., Song, Q., and Du, Z., "Daytime optical turbulence profiling with a profiler of the differential solar limb," *Monthly Notices of the Royal Astronomical Society* **499**(2), 1909–1917 (2020).

[5] Jensen-Clem, R. and Max, C. E., [*Class Astronomy 289: Adaptive Optics and its Applications*], ch. Lecture Note: Basic Concepts of Wavefront Reconstruction, University of California Santa Cruz (2020).

[6] Mansell, J. D., "Control matrices generation for hartmann wavefront sensor adaptive optics," tech. rep., Active Optical Systems, LLC (2009).

[7] Stang, G., [*Linear Algebra and Its Applications*], Academic Press, Inc., 2nd ed. ed. (1980).

[8] Max, C. E., [*Class Astronomy 289: Adaptive Optics and its Applications*], ch. Lecture Note: Error Budgets, and Introduction to Class Projects, University of California Santa Cruz (2020).

[9] Sasiela, R. J., [*Electromagnetic Wave Propagation in Turbulence: Evaluation and Application of Mellin Transforms, 2nd Ed.*], SPIE Press (2007).

[10] Roggemann, M. C. and Koivunen, A. C., "Wave-front sensing and deformable-mirror control in strong scintillation," *J. Opt. Soc. Am. A* **17**(5), 911–919 (2000).

[11] Barchers, J. D., Fried, D. L., Link, D. J., Tyler, G. A., Moretti, W., Brennan, T. J., and Fugate, R. Q., "Performance of wavefront sensors in strong scintillation," in [*Adaptive Optical System Technologies II*], Wizinowich, P. L. and Bonaccini, D., eds., **4839**, 217 – 227, International Society for Optics and Photonics, SPIE (2003).

[12] Engstrom, N. D. and Schmidt, J. D., "Misregistration in adaptive optics systems," in [*Advanced Wavefront Control: Methods, Devices, and Applications VII*], Carreras, R. A., Rhoadarmer, T. A., and Dayton, D. C., eds., **7466**, 74660A, International Society for Optics and Photonics, SPIE (2009).

[13] Heritier, C. T., Esposito, S., Fusco, T., Neichel, B., Oberti, S., Briguglio, R., Agapito, G., Puglisi, A., Pinna, E., and Madec, P.-Y., "A new calibration strategy for adaptive telescopes with pyramid WFS," *Monthly Notices of the Royal Astronomical Society* **481**, 2829–2840 (09 2018).

[14] Hardy, J. W., [*Adaptive Optics for Astronomical Telescopes*], Oxford University Press (1998).

[15] Heritier, C. T., Fusco, T., Oberti, S., Neichel, B., Esposito, S., and Madec, P.-Y., "SPRINT, system parameters recurrent invasive tracking: a fast and least-cost online calibration strategy for adaptive optics," *Monthly Notices of the Royal Astronomical Society* **504**(3), 4274–4290 (2021).

[16] von der Luhe, O. F. H., "Photometric stability of multiconjugate adaptive optics," in [*Advancements in Adaptive Optics*], Calia, D. B., Ellerbroek, B. L., and Ragazzoni, R., eds., **5490**, 617 – 624, International Society for Optics and Photonics, SPIE (2004).

[17] Schmidt, D., Berkefeld, T., Feger, B., and Heidecke, F., "Latest achievements of the MCAO testbed for the GREGOR Solar Telescope," in [*Adaptive Optics Systems II*], Ellerbroek, B. L., Hart, M., Hubin, N., and Wizinowich, P. L., eds., **7736**, 773607, International Society for Optics and Photonics, SPIE (2010).

[18] Tyler, G. A., "Bandwidth considerations for tracking through turbulence," *J. Opt. Soc. Am. A* **11**(1), 358–367 (1994).